

# Lab on a Chip

Accepted Manuscript



This is an *Accepted Manuscript*, which has been through the Royal Society of Chemistry peer review process and has been accepted for publication.

*Accepted Manuscripts* are published online shortly after acceptance, before technical editing, formatting and proof reading. Using this free service, authors can make their results available to the community, in citable form, before we publish the edited article. We will replace this *Accepted Manuscript* with the edited and formatted *Advance Article* as soon as it is available.

You can find more information about *Accepted Manuscripts* in the [Information for Authors](#).

Please note that technical editing may introduce minor changes to the text and/or graphics, which may alter content. The journal's standard [Terms & Conditions](#) and the [Ethical guidelines](#) still apply. In no event shall the Royal Society of Chemistry be held responsible for any errors or omissions in this *Accepted Manuscript* or any consequences arising from the use of any information it contains.

## COMMUNICATION

## Integration of microfluidic chip with a size-based cell bandpass filter for reliable isolation of single cells

Cite this: DOI: 10.1039/x0xx00000x

Hojin Kim,<sup>a</sup> Sanghyun Lee,<sup>a</sup> Jaehyung Lee,<sup>b</sup> and Joonwon Kim\*<sup>a</sup>

Received 00th January 2012,

Accepted 00th January 2012

DOI: 10.1039/x0xx00000x

www.rsc.org/

**We report a simple, efficient microfluidic array system for the reliable isolation of cells. A microfluidic array chip, integrated with a size-based cell bandpass filter, provides the unprecedented capability of organizing single cells from a population containing a wide distribution of sizes.**

Evidence suggests that cellular heterogeneity can be critical to cell fate; however, understanding its full physiological role is challenging.<sup>1-3</sup> Consequently, single-cell analysis is necessary to uncover the role of cellular heterogeneity, which can be masked by conventional ensemble measurement.<sup>4</sup> Several techniques have been established for quantitative single-cell analysis, including flow cytometry,<sup>5</sup> array-based methods,<sup>6-8</sup> and microfluidics.

Microfluidics has emerged as a promising tool for single-cell analysis by providing capabilities of cell handling, environmental controlling, high resolution imaging, and integration of multiple functional components.<sup>9-10</sup> Since the first step in any single-cell analysis is to separate cells of interest, considerable efforts have focused on the isolation of single cells. There are several well-established isolation techniques based on trapping forces, including hydrodynamic,<sup>11-19</sup> dielectrophoretic,<sup>20-21</sup> magnetic,<sup>22</sup> and acoustic trapping.<sup>23</sup> Most of the established single-cell trapping techniques have adopted a hydrodynamic trapping method because of its passive operation and easy parallelization. Hydrodynamic mechanisms are based on dynamic changes in the flow field before and after trapping, which are determined by particle size.<sup>18</sup> Therefore,

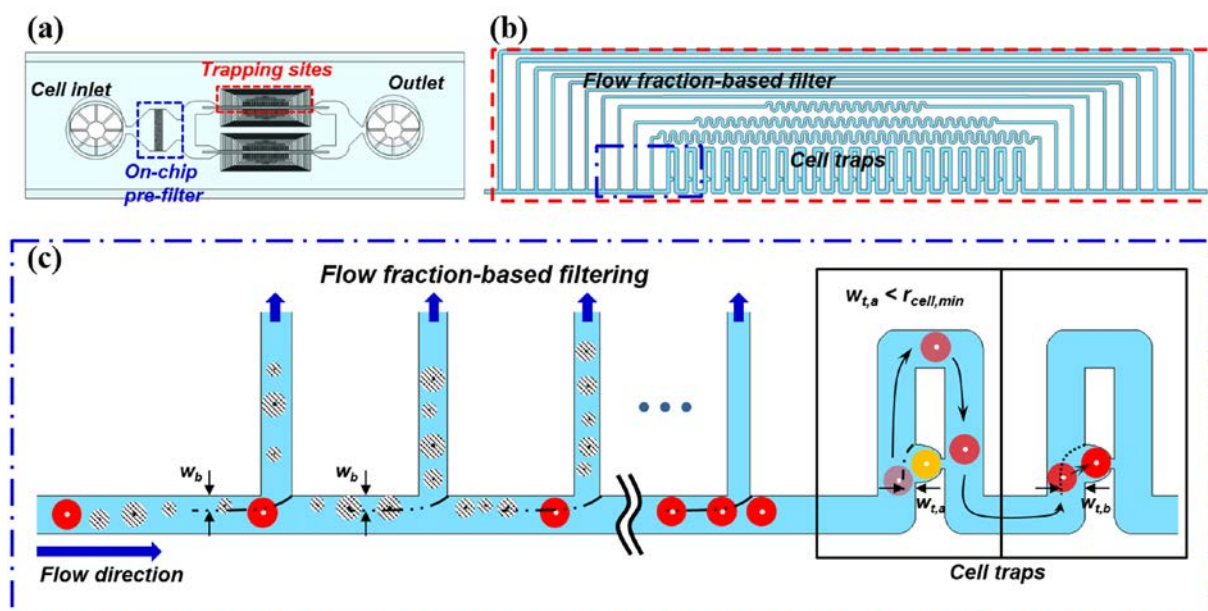


**Fig. 1** (a) A schematic view of the microfluidic single cell array chip. (b) An enlarged schematic view of the trapping site, showing 20 cell traps enclosed by multiple bypass channels. (c) An enlarged schematic view of the area designated by the blue dash-dot box in (b), demonstrating cell filtering and single-cell trapping processes.

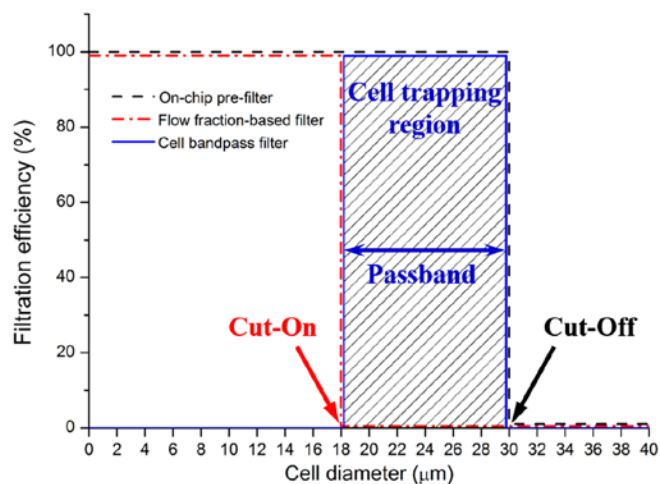


**Fig. 2** Theoretical definition of the size range of cells entering into the cell-trapping region via a cell bandpass filter.

the design of cell trap to coordinate with the size of the target cells is critical for single cell trapping. In previous studies, hydraulic-electric circuit analogy-based analytical methods<sup>18-19</sup> and numerical methods<sup>13</sup> (such as CFD simulation) were used to design the trap; trapping experiments were then conducted to optimize the design based on the applied cell size. Using a well-designed cell-trapping array, Frimat et al. reported remarkable results for trapping single HT29 colon carcinoma cells with an efficiency of ~99%.<sup>14</sup> However, the efficiency for trapping SW480 epithelial cells with an identical microchip decreased considerably (80.6%) and resulted in lower reproducibility. This is most likely due to the larger size distribution of SW480 cells ( $\pm 3.0$   $\mu\text{m}$ ) compared to that of HT29 cells ( $\pm 1.1$   $\mu\text{m}$ ), although the two cell types have similar average diameters (14.6  $\mu\text{m}$  for SW480 cells vs. 14.7  $\mu\text{m}$  for HT29 cells). For SW480 cells, an insufficient increase in the hydraulic resistance of the cell trap, due to trapping of the smallest cells, led to trapping of additional cells.<sup>18</sup> The results indicate that single-cell array techniques utilizing dynamic flow have an inherent performance limitation in single-cell trapping, since many biological cell types have polydisperse distributions.

To address the intrinsic problem, we present a novel microfluidic approach for the reliable arraying of single cells utilizing an on-chip size-based cell bandpass filter. The key principle to this approach is not the optimization of a cell trap design, but rather, the regulation of the size distribution of cells, from a bulk cell suspension, entering trapping sites. The proposed approach revealed that the trapping efficiency of single cells varied considerably with the band range (i.e., size ranges of sorted cells) of the cell bandpass filter. The trapping efficiency increased from 77.6% to 99.2% for the mouse fibroblast 3T3-J2 cell line and from 40.6% to 95.8% for the MC3T3-E1 pre-osteoblast cell line. In addition, intracellular esterase activity was observed using the single-cell arrays, demonstrating capability for quantitative real-time monitoring of single cells.

The polydimethylsiloxane (PDMS)-glass hybrid microfluidic single-cell array chip is fabricated via a standard soft lithography technique (Fig. 1a). The chip is composed of an on-chip pre-filter to prevent the inflow of large cells that could potentially clog the microchannel, as well as four parallel trapping sites. The chip also consists of a simple design with one inlet and one outlet, facilitating an easy operation. Each trapping site consists of 20 cell traps that are

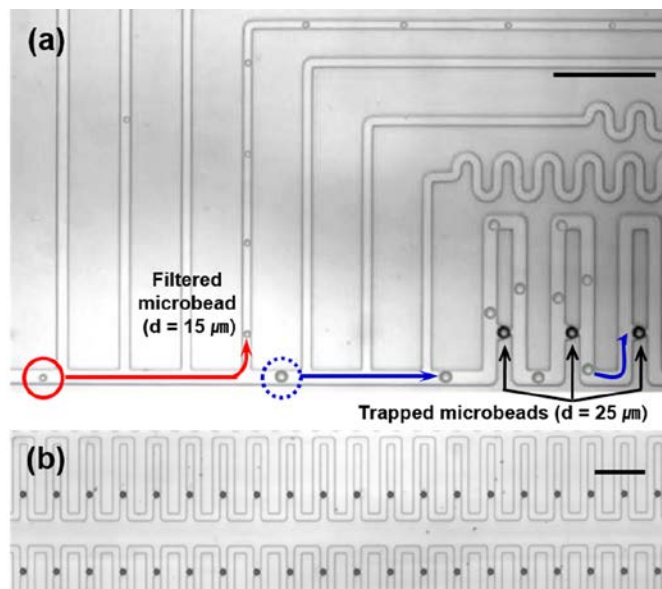


**Fig. 3** (a) Demonstration of the filtering process for a 15- $\mu\text{m}$  bead via the flow fraction-based cell filter, and the trapping process of a 25- $\mu\text{m}$  bead. (b) A single-cell array containing 25- $\mu\text{m}$  beads. Scale bar: 200  $\mu\text{m}$ .

enclosed by multiple bypass channels that act as a size-based cell filter based on flow fraction (Fig. 1b). Figure 1c demonstrates the mechanism for the trapping site to enhance the trapping efficiency of heterogeneous-sized cells. Cells with radii smaller than a specific size ( $w_b$ ) are removed via flow fraction through the filter channels that intersect the main channel,<sup>24</sup> whereas larger cells enter into the meander-shaped cell traps. These cells are then sequentially trapped into empty cell traps upstream, based on the dynamic change of hydraulic resistance.

Based on our previous theoretical analysis for determining single bead trapping conditions,<sup>18</sup> the width ( $w_{t,a}$ ) of the stream after trapping a single cell should be less than the radius ( $r_{cell,min}$ ) of the smallest cell among influent cells, thereby preventing additional trapping of sequential cells into the cell trap. In addition, the width ( $w_{t,b}$ ) of the stream in an empty trap should be large enough to introduce cells efficiently into the cell trap. The widths  $w_{t,b}$  and  $w_{t,a}$  of the trapping stream should therefore be designed depending on the cell size, as follows:

$$w_{t,a} < r_{cell} < w_{t,b} \quad (\text{ineqn. 1})$$

Based on our previous theoretical study to determine the width values  $w_{t,b}$  and  $w_{t,a}$ ,<sup>25</sup> this inequation is invalid for most biological cells due to their Gaussian size distribution. Moreover, cell size distribution varies with cell types, signifying the limitation of the microfluidic approach through design optimization. Therefore, our strategy was to narrow the size distribution of influent cells into the cell trapping region via the cell bandpass filter. Fig. 2 shows the mechanism for the delivery of cells, ranging between two sizes, to the cell-trapping region using the bandpass filter. The space between the pillars of the on-chip pre-filter and the width ( $w_b$ ) of the stream entering into the flow fraction-based cell filter regulate the maximum (i.e., half of the cut-off size) and minimum (i.e., half of the cut-on size) values of  $r_{cell}$ , respectively. To evaluate the effect of the band range on the trapping efficiency of single cells, we designed band ranges of 0–30  $\mu\text{m}$ , 16–30  $\mu\text{m}$ , and 18–30  $\mu\text{m}$ . Details of the

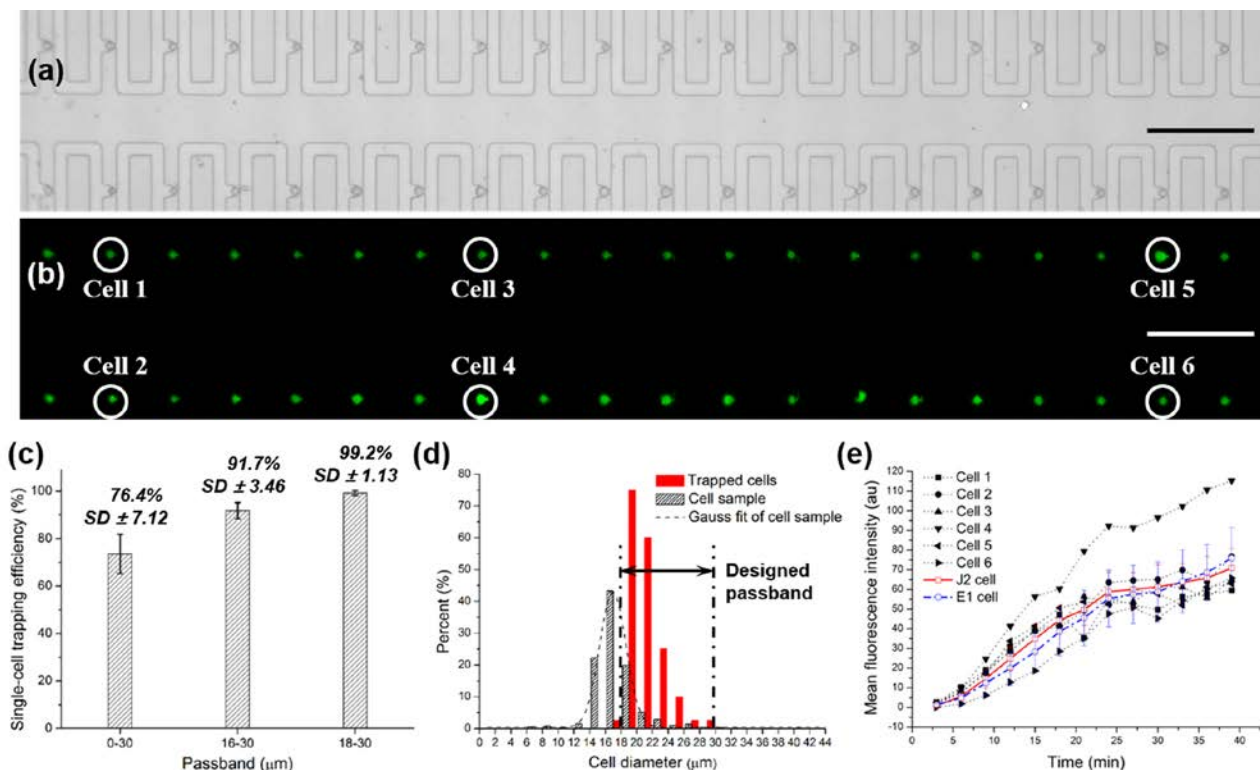


**Fig. 4** (a) A single-cell array consisting of 40 cells with a trapping efficiency of 100%. Scale bar: 200  $\mu\text{m}$ . (b) A fluorescence image of viable cells. Scale bar: 200  $\mu\text{m}$ . (c) The effect of a band range on the trapping efficiency ( $n = 80$ ; triplicate) of single cells. The trapping efficiency of single cells was defined as the percentage of traps occupied with a single cell relative to the total number of cell traps after the arraying process.<sup>17</sup> (d) Size distribution profiles of 3T3-J2 cells ( $n = 670$ ; hatched column) and filtered cells ( $n = 40$ ; red solid column) via the cell bandpass filter with the 18–30  $\mu\text{m}$  passband. (e) Mean fluorescence intensity profiles of six individual cells (represented by circles in Fig. 4b), and the average fluorescence intensity measurements for 3T3-J2 ( $n = 80$ ) and MC3T3-E1 ( $n = 80$ ) cells over time.

design process and the chip dimensions are provided in ESI†.

Using two different sizes of microbeads (15 and 25  $\mu\text{m}$  in diameter), the filtering capability of the flow fraction-based cell filter and the trapping capability of the cell trap were examined. A droplet of a bead mixture was applied to the chip inlet and mobilized through the microchannel via negative pressurization that was applied at the outlet. This procedure allows multiple experiments to be simultaneously performed using separate chips. To quantitate the filtering and trapping efficiencies, three individual chips with a band range of 18–30  $\mu\text{m}$  were tested. Fig. 3a shows a superimposed image of bead filtering and trapping processes. All of the beads passed through the pre-filter; the 15  $\mu\text{m}$  beads were then filtered through multiple bypass channels, whereas the 25  $\mu\text{m}$  beads entered the trap and were trapped sequentially as shown in Fig. 3b (refer to ESI† Movie 1). The results show that the filtering and trapping efficiencies were both 100.

For a more detailed investigation of filtering and trapping using this microfluidic chip, biological cell types with a Gaussian size distribution were tested: 3T3-J2 cells ( $17.5 \pm 3.0 \mu\text{m}$ ; min.:  $\sim 7.0 \mu\text{m}$ , max.:  $\sim 41.0 \mu\text{m}$ ) and MC3T3-E1 cells ( $15.2 \pm 2.1 \mu\text{m}$ ; min.:  $\sim 9.4 \mu\text{m}$ , max.:  $\sim 24.8 \mu\text{m}$ ). All microfluidic chips were sterilized by autoclaving prior to use.<sup>26</sup> Cells were introduced into the chip by applying low negative pressure ( $-2 \text{ kPa}$ ) to prevent the flow of cells larger than the cut-off size, which could be caused by shear stress-induced cell deformation under high pressure conditions; cell traps were occupied within a few minutes of flow. After cell arraying, a viability assay was carried out. A green fluorescent signal in trapped

cells demonstrates that the arraying process was favorable to the cells (Fig. 4b).<sup>20</sup> The trapping efficiency of single cells varied considerably depending on the band range (Fig. 4c); the efficiencies for 3T3-J2 cells were 73.5%, 91.7%, and 99.2% for 0–30  $\mu\text{m}$ , 16–30  $\mu\text{m}$ , and 18–30  $\mu\text{m}$  passband filters, respectively. The frequency of multiple trapping events (i.e., trapping of multiple cells) decreased with an increase in the cut-on size (i.e., from 0 to 18  $\mu\text{m}$ ). The filter with a cut-on size of 18  $\mu\text{m}$  efficiently prevented the inflow of the smallest cells into the cell-trapping area by removing them via flow fraction, whereas low trapping performance and reproducibility (i.e., large standard deviation) were observed without a flow fraction-based filter. These experimental results support our claim that regulating the size distribution of cells is crucial to single-cell trapping. To reinforce this claim, an arraying experiment was performed using MC3T3-E1 cells with a smaller size than that of 3T3-J2 cells (details on the size distribution of the two cell types are provided in Fig. S1 in ESI†). Single-cell trapping efficiency using the 0–30  $\mu\text{m}$  passband filter was 40.6%, while the efficiency using the 18–30  $\mu\text{m}$  passband filter was 95.8%. This demonstrates that the design of cell trap was inadequate for trapping single MC3T3-E1 cells. However, considerable enhancement in trapping efficiency was obtained with on-chip bandpass filtering. Based on the arraying test of these two different cell types, it is postulated that reliable and efficient single-cell arraying for other biological cells could also be achieved using the microfluidic array chip with an 18–30  $\mu\text{m}$  passband. A microfluidic chip with a larger cut-on size (i.e., above 18  $\mu\text{m}$ ) would also provide high trapping performance. However,

this would limit the number of cell types that could be applied because the passband would be narrowed. Fig. 4d demonstrates highly efficient filtering of 3T3-J2 cells using the 18–30  $\mu\text{m}$  bandpass filter. The results show that size distribution of trapped cells was clearly confined by the designed band range, while the 3T3-J2 cell sample had a Gaussian distribution.

Using each single cell array of 3T3-J2 and MC3T3-E1 cells, intracellular enzymatic analysis was conducted to demonstrate the applicability of the chip to real-time, parallel, single-cell monitoring under continuous flow conditions, which are normally required to promote chemical stimuli. Immediately after cell trapping, 2  $\mu\text{M}$  Calcein acetoxymethyl ester (Calcein AM) solution was continuously infused into the chip under application of negative pressure (-2 kPa). In the presence of intracellular esterase activity, non-fluorescent cell-permeant Calcein AM is converted to fluorescent Calcein. Fig. 4e shows the fluorescence intensity profiles of six individual 3T3-J2 cells (indicated in Fig. 4b) and the average measurement of fluorescence intensities for 3T3-J2 and MC3T3-E1 cells over time. Variation in fluorescence intensity among individual cells was observed. This intensity data could be converted to quantify the abundance of intracellular carboxylesterases.<sup>27</sup>

## Conclusions

In summary, we developed a cell bandpass filter integrated with a microfluidic chip containing a single-cell array. In contrast to conventional approaches that involve the optimization of the cell trap design, this novel on-chip filtering and arraying approach provided an extremely efficient and reliable arraying performance for two different cell types with the same design. Based on the experiments and methods presented, other cells types can be isolated and studied at the single-cell level using the proposed chip. The proposed trapping site contains a network comprised of a single channel, and thus can be easily integrated with other microfluidic components (e.g., an upstream gradient generator) for numerous single-cell applications. Potential future projects for this microfluidic chip involve the sorting and arraying of cells of interest from a cell mixture using a well-designed passband, (e.g., tumor cells circulating with blood cells). We believe that the proposed chip will be useful for single-cell analysis requiring reliable arraying of individual cells.

## Acknowledgements

This research was supported by BioNano Health-Guard Research Center funded by the Ministry of Science, ICT & Future Planning (MSIP) of Korea as Global Frontier Project (H-GUARD\_2014M3A6B2060526) and Basic Research Program through the National Research Foundation of Korea (NRF) funded by the Ministry of Education, Science and Technology (2012R1A1A2006305).

## Notes and references

<sup>a</sup>Department of Mechanical Engineering, Pohang University of Science and Technology, San 31, Pohang, Kyungbuk, Republic of Korea, 790-784. Fax: +82-54-279-2960; Tel: +82-54-279-2185; E-mail: Joonwon@postech.ac.kr

<sup>b</sup>Stratio, Inc., 998 Hamilton Ave., Menlo Park, CA 94025.

† Electronic Supplementary Information (ESI) available: Movie 1, filtering and sequential trapping processes of a bead mixture; the design

and dimensions of the microfluidic single cell array chip with a band range of 18–30  $\mu\text{m}$ . See DOI: 10.1039/c000000x/

- 1 T. J. Perkins and P. S. Swain, *Molecular systems biology*, 2009, **5**, 326.
- 2 W. M. Weaver, P. Tseng, A. Kunze, M. Masaeli, A. J. Chung, J. S. Dudani, H. Kittur, R. P. Kulkarni and D. Di Carlo, *Current opinion in biotechnology*, 2014, **25**, 114-123.
- 3 V. Lecaulet, A. K. White, A. Singhal and C. L. Hansen, *Current opinion in chemical biology*, 2012, **16**, 381-390.
- 4 N. M. Toriello, E. S. Douglas, N. Thaitrong, S. C. Hsiao, M. B. Francis, C. R. Bertozzi and R. A. Mathies, *Proceedings of the National Academy of Sciences of the United States of America*, 2008, **105**, 20173-20178.
- 5 P. O. Krutzik and G. P. Nolan, *Nature methods*, 2006, **3**, 361-368.
- 6 J. R. Rettig and A. Folch, *Analytical chemistry*, 2005, **77**, 5628-5634.
- 7 M. Hosokawa, A. Arakaki, M. Takahashi, T. Mori, H. Takeyama and T. Matsunaga, *Analytical chemistry*, 2009, **81**, 5308-5313.
- 8 Y. Liu, B. Kirkland, J. Shirley, Z. Wang, P. Zhang, J. Stembridge, W. Wong, S. Takebayashi, D. M. Gilbert, S. Lenhert and J. Guan, *Lab on a chip*, 2013, **13**, 1316-1324.
- 9 R. N. Zare and S. Kim, *Annual review of biomedical engineering*, 2010, **12**, 187-201.
- 10 H. Yin and D. Marshall, *Current opinion in biotechnology*, 2012, **23**, 110-119.
- 11 D. Di Carlo, L. Y. Wu and L. P. Lee, *Lab on a chip*, 2006, **6**, 1445-1449.
- 12 D. Wlodkovic, S. Faley, M. Zagnoni, J. P. Wikswo and J. M. Cooper, *Analytical chemistry*, 2009, **81**, 5517-5523.
- 13 S. Kobel, A. Valero, J. Latt, P. Renaud and M. Lutolf, *Lab on a chip*, 2010, **10**, 857-863.
- 14 J. P. Frimat, M. Becker, Y. Y. Chiang, U. Marggraf, D. Janasek, J. G. Hengstler, J. Franzke and J. West, *Lab on a chip*, 2011, **11**, 231-237.
- 15 J. Chung, Y. J. Kim and E. Yoon, *Applied physics letters*, 2011, **98**, 123701.
- 16 A. Lawrenz, F. Nason and J. J. Cooper-White, *Biomicrofluidics*, 2012, **6**, 024112.
- 17 R. D. Sochol, M. E. Dueck, S. Li, L. P. Lee and L. Lin, *Lab on a chip*, 2012, **12**, 5051-5056.
- 18 H. Kim, S. Lee and J. Kim, *Microfluidics and Nanofluidics*, 2012, **13**, 835-844.
- 19 D. Jin, B. Deng, J. X. Li, W. Cai, L. Tu, J. Chen, Q. Wu and W. H. Wang, *Biomicrofluidics*, 2015, **9**, 014101.
- 20 J. Voldman, M. L. Gray, M. Toner and M. A. Schmidt, *Analytical chemistry*, 2002, **74**, 3984-3990.
- 21 Z. Zhu, O. Frey, D. S. Ottoz, F. Rudolf and A. Hierlemann, *Lab on a chip*, 2012, **12**, 906-915.
- 22 K. Ino, M. Okochi, N. Konishi, M. Nakatochi, R. Imai, M. Shikida, A. Ito and H. Honda, *Lab on a chip*, 2008, **8**, 134-142.
- 23 X. Ding, S.-C. S. Lin, B. Kiraly, H. Yue, S. Li, I.-K. Chiang, J. Shi, S. J. Benkovic and T. J. Huang, *Proceedings of the National Academy of Sciences*, 2012, **109**, 11105-11109.
- 24 M. Yamada and M. Seki, *Lab on a chip*, 2005, **5**, 1233-1239.
- 25 H. Kim and J. Kim, *Microfluidics and nanofluidics*, 2014, **16**, 623-633.

## Journal Name

- 26 Y. Shin, S. Han, J. S. Jeon, K. Yamamoto, I. K. Zervantonakis, R. Sudo, R. D. Kamm and S. Chung, *Nature protocols*, 2012, **7**, 1247-1259.
- 27 D. Di Carlo, N. Aghdam and L. P. Lee, *Analytical chemistry*, **2006**, **78**, 4925-4930.